

## Special Article

# Progressive collapsing foot deformity: how to use new knowledge in developing countries

Nacime Salomao Barbachan Mansur<sup>1,2</sup> , Kevin Dibbern<sup>3</sup> , César de César Netto<sup>4</sup> 

1. Medstar Orthopedic Institute, MedStar Union Memorial Hospital, Baltimore, United States.

2. Federal University of Sao Paulo, Department of Orthopedics and Traumatology, Sao Paulo, Brazil.

3. Orthopaedic & Rehabilitation Engineering Center, Marquette University, Milwaukee, United States.

4. Department of Orthopaedic Surgery, Division of Foot and Ankle Surgery, Duke University Health System, Durham, United States.

## Abstract

The 2019 progressive collapsing foot deformity (PCFD) consensus did not only change the disease nomenclature and provided a new classification for the condition formerly known as flatfoot deformity. It was also the pinnacle of a revolution in the field in terms of knowledge and clinical perspectives. The use of advanced imaging, such as weight-bearing computed tomography, three-dimensional algorithms, and magnetic resonance, expanded the way we understand peritalar subluxation and how we can address it. However, much of these improvements felt short in terms of global reproducibility due to economic restraints. The objective of this review study is to present PCFD new concepts through the lens and realities of developing countries, considering their potentially limited access to novel technologies.

**Level of Evidence V; Expert opinion.**

**Keywords:** Flatfoot; Tomography; Cone-Beam Computed Tomography; Disruptive Technology; Low Cost Technology; Developing Countries.

## Introduction

Progressive collapsing foot deformity (PCFD) was the name chosen to better describe what was previously termed flatfoot by a consensus of world specialists in the disease through a series of articles, in 2020<sup>(1,2)</sup>. The nomenclature would solve some of the problems associated with adult acquired flatfoot deformity, such as the fact it might occur outside the adult scope and present congenital features, besides not being a variation of normality<sup>(1,3,4)</sup>. Setting these concepts and establishing the posterior tibial tendon as the main driver of the disease was only possible due to an ocean of knowledge produced in the years previous to the consensus<sup>(5,6)</sup>. What was produced in the following years substantiated and expanded these principles around PCFD<sup>(7,8)</sup>, and much of this new knowledge was possible with the advent of the weight-bearing computed tomography (WBCT)<sup>(9,10)</sup>. By assessing the

foot and ankle under physiological stress, relations among structures and their environment were redefined due to this clearer portrayal of the local anatomy, including coronal and three-dimensional (3D) assessments<sup>(11-13)</sup>. This technology allowed further development of bone segmentation and 3D mappings, increasing our understanding on how components interact in the normal and PCFD scenarios<sup>(14,15)</sup>. Lately, the clinical applicability of these findings has been putted into test, and results are encouraging<sup>(16)</sup>.

Contrary to what is expected from a scientific product, many of the treatment plans elaborated were not able to reach practice globally, especially in developing countries with economic restraints. This review study aims to report the scientific advancements made in PCFD over the last years while trying to implement these ideas in locations with limited access to technology.

Study performed at the Medstar Orthopedic Institute, MedStar Union Memorial Hospital, Baltimore, United States.

**Correspondence:** Nacime Salomao Barbachan Mansur. Department of Orthopaedic Surgery, MedStar Union Memorial Hospital, 201 E, University Pkwy, Baltimore, MD 21218. **Email:** [nacimesbm@gmail.com](mailto:nacimesbm@gmail.com). **Conflicts of interest:** none. **Source of funding:** none. **Date received:** April 24, 2024. **Date accepted:** April 24, 2024. **Online:** April 30, 2024.

**How to cite this article: Mansur NS, Dibbern K, Netto CC. Progressive collapsing foot deformity: how to use new knowledge in developing countries. J Foot Ankle. 2024;18(1):12-20.**



### The Concept of Peritalar Subluxation (PTS)

The concept is not new, being introduced by Sangeorzan et al. more than two decades ago and using conventional weight-bearing radiographs (WBRs) and non-weightbearing computed tomography (CT)<sup>(5,17)</sup>. In PCFD/flatfoot, the talus would stay in a fixed position while the structures around it would progressively subluxate, moving in external rotation, eversion, and dorsiflexion (Figure 1)<sup>(6)</sup>. Although intuitively being an ongoing aspect of a pathological process, PTS was also found to be extremely accurate in diagnosing PCFD, also being reliable for assessment of treatment success<sup>(16,18)</sup>.

Ananthakrishnan et al. used the overlap of posterior facets of the talus and calcaneus as a marker of PTS to demonstrate the difference between flatfeet and controls (0.92 vs. 0.68;  $p = 0.0066$ )<sup>(17)</sup>. Later, de Cesar et al. explored the middle facet of the subtalar joint and found this subluxation has a high

accuracy (>17.9%, with 100% specificity and 96.7% sensitivity; AUC = 0.99) and presents as an earlier mark (middle vs. posterior difference: 17.7%) for PCFD diagnosis (Figure 2)<sup>(18,19)</sup>. Whilst most of these findings were established by WBCT, which could be of limited access in developing countries, concepts can still be appreciated in simulated WBCT and WBR<sup>(20,21)</sup>.

Sinus tarsi impingement (STI) and subfibular impingement (SFI) are also important clinical and radiographic manifestations of PTS<sup>(14,22)</sup>. They probably represent prognostic factors too, STI being a sign of symptom onset and SFI, an indication of more pronounced and advanced PTS<sup>(16)</sup>. Several studies demonstrated a correlation between impingement and PCFD diagnosis, function, pain, deformity severity, and soft tissue impairment<sup>(15,16,22,23)</sup>. Recognizing an STI or SFI in the clinical setting is crucial and does not require advanced imaging<sup>(23,24)</sup>. Physical examination and conventional WBR, including a hindfoot alignment view, are adequate and inexpensive<sup>(25,26)</sup>.

It is important to differentiate STI from subtalar arthritis, since they can determine distinct treatments (joint sparing vs. fusion)<sup>(27-29)</sup>. In STI, alongside with localized pain at the sinus tarsi, radiographs show a direct contact between the lateral process of the talus and the Gissane angle in the calcaneus<sup>(22)</sup>. If available, a magnetic resonance imaging can show indirect signs, such as bone edema, subchondral cysts, or erosion of the lateral process and Gissane<sup>(23)</sup>. Arthritis has a more diffuse clinical pattern and also significant loss of subtalar joint space,

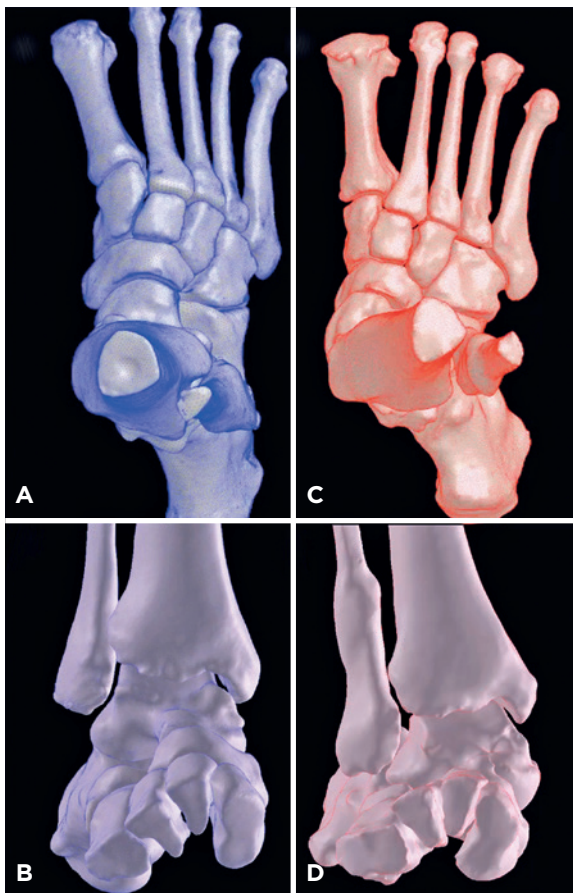


**Figure 1.** Three-dimensional weight-bearing computed tomography reconstruction from a patient with neutral/physiological alignment (blue; A and B) and progressive collapsing foot deformity (red; C and D). Axial (A and C) and coronal (B and D) views show signs of peritalar subluxation, such as external rotation and eversion of the subtalar joint, midtarsal external rotation and translation, and subtalar and subfibular impingement.



**Figure 2.** Coronal weight-bearing computed tomography images showing middle facet subluxation (A) and posterior facet subluxation (B) in patients with progressive collapsing foot deformity. The red circle highlights the area of interest and where the subluxation is measured.

which might be not so easy to assess with the overlapping of bones (Figure 3)<sup>(24,30)</sup>. A combination of diagnostic modalities might provide answers in challenging cases<sup>(4,28)</sup>.

### Weight-bearing Computed Tomography (WBCT)

The development of WBCT changed the PCFD understanding substantially<sup>(21)</sup>. Not only PTS and joint interaction became clearer, but other aspects of the disease were also highlighted<sup>(1,11,31)</sup>. The new consensus classification incorporated the idea of different deformity patterns combining into a PCFD presentation (Table 1)<sup>(1,32)</sup>. Much of the classes are easily recognizable clinically and radiographically, such as A (hindfoot valgus) and E (ankle instability). However, as previously stated, class D (PTS) is better appreciated by WBCT<sup>(31)</sup>. The identification of classes B (midfoot abduction) and C (medial column instability), in particular, can be incremented with the technology due to its

multiplane capability<sup>(31)</sup>. Instability of the tarsometatarsal or naviculocuneiform joints, in the form of plantar gapping, dorsal subluxation, or arthritis, can change the therapeutic approach of PCFD<sup>(33-35)</sup>. Foot tripod reestablishment through a medial longitudinal arch stabilization procedure directed to the apex of the deformity is a fundamental step of the reconstruction plan<sup>(36-38)</sup>. Again, the rational use of a careful clinical assessment combined with WBR (and, eventually, simulated WBCT) to assess classes B and C can bring plentiful information for the decision making<sup>(39,40)</sup>.

Multiple imaging acquisition by WBCT also allowed the development of different software to analyze the obtained data<sup>(20,41,42)</sup>. One of the first and most impactful of these is the Foot and Ankle Offset (FAO)<sup>(43)</sup>. The 3D relation between the center of the ankle and the foot tripod was introduced by Lintz et al. with the use of WBR, at first<sup>(44)</sup>. The Torque Ankle Lever Arm System (TALAS®; CurveBeam™, LLC, Warrington,



**Figure 3.** Progressive collapsing foot deformity patient with sinus tarsi impingement. Lateral weight-bearing radiograph (A) shows the lateral facet of the talus touching the crucial angle of Gissane in the calcaneus. Assessment of the joint space is significantly hindered by the apposition of bones. The technique illustrates the contact between bones as well as cystic changes (B) and sclerosis secondary to the impingement. Other indirect signs of STI can be seen in the magnetic resonance imaging, such as bone edema, subchondral cysts, and local synovitis (D).

**Table 1.** Progressive collapsing foot deformity consensus classification enabling a combination of classes with flexible (stage I) or rigid (stage II) presentations

Types	Stage I: Flexible Deformity type/location	Stage II: Rigid Consistent clinical/radiographic findings
Class A	Hindfoot valgus	Hindfoot valgus alignment Increased HMA, HAA, and FAO
Class B	Midfoot/forefoot abduction	Decreased talar head coverage Increased TNCA Presence of STI
Class C	Forefoot varus/medial column instability	Increased TFMA Plantar gapping at first TMT/NC joints Clinical forefoot varus
Class D	Peritalar subluxation/dislocation	Significant subtalar joint subluxation SFI
Class E	Ankle instability	Valgus tilting of the ankle

HMA: hindfoot moment arm; HAA: hindfoot alignment angle; FAO: foot and ankle offset; TNCA: talonavicular coverage angle; STI: sinus tarsi impingement; TFMA: talus-first metatarsal angle; TMT: tarsometatarsal joint; NC: naviculocuneiform joint; SFI: subfibular impingement.

PA) program allowed FAO to be obtained in a semi-automatic manner, by clicking at the most distal voxel (aspect) of the first metatarsal head, followed by the most distal voxel of the fifth metatarsal head and the most distal voxel of the calcaneus posterior tuberosity<sup>(45,46)</sup>. Those three points generate the foot tripod<sup>(44,46)</sup>. Finally, the most central point of the talar body is obtained and the amount of this point deviation considering the center of the tripod is automatically measured by a percentage (Figure 4)<sup>(47)</sup>. Normal values range between -0.6% and 5.2% (mean: 2.3%), as positive values above 5.2% indicate valgus, and negative values below -0.6%, varus<sup>(45,46)</sup>. The FAO has been demonstrating high reliability rates (>0.97), diagnostic values (>4.6%: 100% specificity and 89.2% sensitivity), and clinical correlations as a surrogate for overall foot and ankle alignment<sup>(13,48-50)</sup>. Manual measurement using simulated WBCT or even WBR is possible in situations where a WBCT or the software are not available (Figure 4)<sup>(44-46)</sup>.

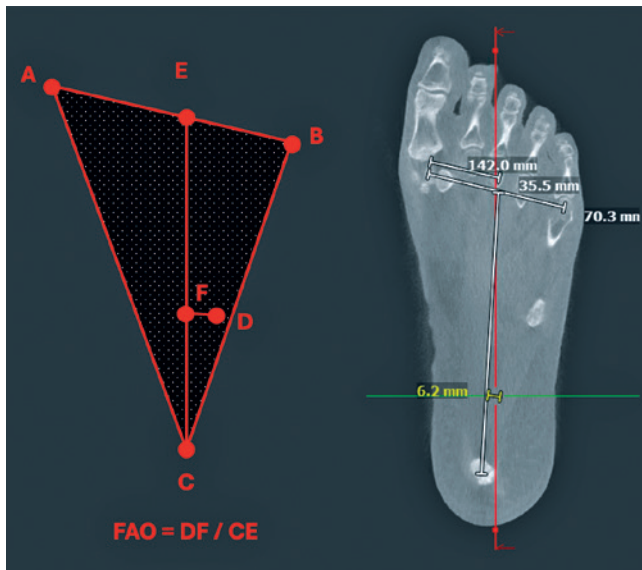


**Figure 4.** Measuring the foot and ankle offset without semi-automatic software. In this case, a conventional computed tomography with simulated weightbearing was used. The most distal aspect of the first metatarsal is determined in the three computed tomography planes and marked (point A). Using the three planes, the most distal aspect of the fifth metatarsal is obtained (point B). Next, the most distal aspect of the calcaneus is found (point C). The mid-distance between points A and B ( $70/2 = 35$ ) is marked as point E. A line is drawn between points E and C and the distance is measured (142 mm). The projection of the center of the talus to the tripod plane is established as point D. A perpendicular line connecting point D with the CE line (point F at the line) represents the DF distance (6.2 mm). Line F would be a perfect alignment of the talus over the center of the tripod. The FAO can be obtained by dividing DF (6.2) by CE (142); in the represented case, 0.0436, or 4.36%, of talar deviation from the point F or the central tripod line.

South America currently holds only two WBCT equipment in operation, while it is still scarce in Africa and Asia. Nonetheless, much of the PCFD concepts developed or expanded with WBCT have strong clinical and radiographic correspondence<sup>(20)</sup>. Classes, stages, and presentations can be clearly identified using traditional approaches. As many of the ideas and advancements brought by these apparatuses, FAO can be employed with creativity, using the concepts introduced by the original authors.

### Three-dimensional (3D) Algorithms

Segmentation is not a novelty when it comes to imaging assessment and medical applications<sup>(51,52)</sup>. Image acquisition and software developments were fundamental to the thriving of this technology, allowing 3D WBCT mapping algorithms to be established<sup>(53,54)</sup>. The software captures the images from the WBCT file, creating a 3D isosurface of the bone tissue<sup>(55)</sup>. In order to obtain a patient-specific shape, deformable shape models are used by the program, which also automatically generates landmarks and bone axis<sup>(56)</sup>. Bone segmentation can then be used to perform simple, automatic angular and linear measurements reliably (ICCs: >0.972) and faster (97%)<sup>(53,57)</sup>. Mostly, a more comprehensive assessment of structural interaction in a 3D approach is possible using distance and coverage mapping<sup>(15,56,58)</sup>.

Many of the PCFD concepts proposed in the last decades were substantiated using this advanced technology<sup>(58,59)</sup>. Studies were able to fully characterize PTS through changes on joint coverage, bone positioning, and distancing<sup>(57,60)</sup>. Middle facet subluxation (46.6% of uncoverage), sinus tarsi impingement (98% increase in coverage), and subfibular impingement (17 of 20 patients) were more objectively and extensively appreciated using maps of coverage and distance for the specific areas<sup>(15)</sup>. A direct clinical application of the same concepts was later demonstrated by de Cesar et al. when showing changes in coverage and distance by 3D mapping in patients operated for PCFD joint-sparing procedures (Figure 5)<sup>(16)</sup>. A direct correlation among improvement in patient reported outcomes (PROs), improvement in facet coverage (middle facet and PCS;  $p = 0.030$ ), and impingement (SFI and PROMIS;  $p = 0.020$ ) was established. In this study, the FAO improvement also affected PROs significantly (i.e.,  $R^2 = 0.35$  for VAS), showing that the correction of overall alignment, joint coverage, and extra-articular impingements (STI and SFI) have a positive effect on clinical results.

Although challenging to be obtained in low economic environments, 3D WBCT mapping algorithm conceptions help not only by driving innovation in the field, but also allows a more contemplative metric<sup>(16,59)</sup>. Many of the software being developed for segmentation and 3D analysis are able to get data from simulated WBCT and, in some extent, WBR. Imaging from normal, pathological, and cadaveric samples are feeding artificial neural networks that might be able to translate data from different modalities. As the orthopedic industry evolves and invests in this technology, more are the chances of these software being offered freely to providers around the globe.



### Surgical Planning and Interventions

Application of basic concepts in segmentation and 3D WBCT algorithms allowed researchers and engineers to develop surgical planning tools in programs<sup>(61-63)</sup>. It is possible to feed the software with preoperative WBCT images and simulate the effect of isolated or combined osteotomies on specific measurements and on the overall foot alignment (Figure 6)<sup>(64-66)</sup>. As discussed, artificial intelligence is supplied with cases and studies, making 3D preoperative plans increasingly more consistent<sup>(63,67)</sup>. Although this technology will not replace the surgeon’s insights and experience, it will potentially add good information when making intraoperative decisions, such as the desired amount of displacement in a calcaneal osteotomy, the size of an wedge for a midfoot osteotomy, or the need for additional soft tissue procedures<sup>(63,67)</sup>. Again, these are not indispensable steps when planning PCFD reconstruction, but there is hope that these software become widely available in the future, with the ability to translate data from simulated WBCT and WBR<sup>(68)</sup>.

Technical surgical aspects have not changed much in the last decades, even though advancements in soft tissue reconstruction are promising<sup>(69,70)</sup>. There is a tendency of

leaving the posterior tibial tendon intact whenever possible<sup>(23,71,72)</sup>. Placing the calcaneus under the tibial axis and reestablishing the foot tripod are still the main goals of PCFD bone reconstruction, while avoiding hypercorrection<sup>(4,28,37,73)</sup>. The importance of the first ray and medial column in regaining triple foot support has been highlighted in the last years (Figure 7)<sup>(24,34-36)</sup>. A short or insufficiently plantarflexed first ray/medial column might not be enough to derotate the hindfoot, helping to correct PTS<sup>(74,75)</sup>. On the other spectrum of the disease – rigid deformities –, well-aligned triple arthrodesis is still found to be mandatory for good outcomes and to protect the ankle joint<sup>(39,76)</sup>. Moreover, as total ankle replacements continue to evolve, they became a viable option when treating class E deformities in a PCFD setting<sup>(77,78)</sup>.

New implants are constantly developed to treat the different aspects and presentations of PCFD. Still, they lack clinical superiority over the traditional implants available in developing places<sup>(79-81)</sup>. Allograft pre-molded wedges can be substituted by metal or autograft<sup>(81)</sup>. Free tendon graft or suture material might replace expensive suture tapes and anchors<sup>(77,78,82,83)</sup>. The creativity of the developing world surgeon in specific situations is also an important factor when operating specific cases.

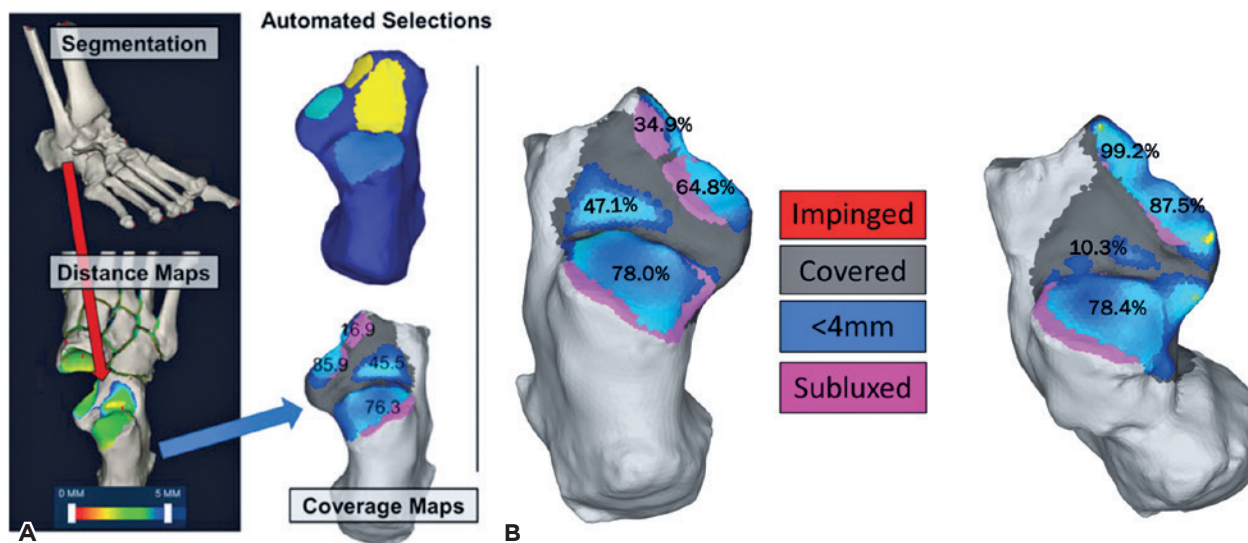


**Figure 5.** Three-dimensional weight-bearing computed tomography algorithms starts with bone segmentation (A), providing anatomical displays of the desired interaction - in this case, the subtalar joint. Vertical vectors between talus and calcaneus are obtained, portraying distance and coverage maps. Distance is portrayed in millimeters, red colors representing areas with smaller distances (arthritis or impingement) and green/blue, greater distances. Coverage is displayed using color diagrams for these vectors that characterize how much the structures are close to or with no contact with each other. Red represents contact between bones (impingement), blue symbolizes distances bellow 4 mm (physiological coverage), gray denotes coverage with distances over 4 mm, and pink indicates no coverage (subluxation). Example of a Three-dimensional weight-bearing computed tomography coverage map (B) in progressive collapsing foot deformity preoperatively and postoperatively. Before surgery, sinus tarsi have signs of impingement (more coverage: 47%, less distance) and medial and anterior facets have a significant subluxation (34% and 64% of coverage, respectively). After joint-sparing procedures, facets recover much of the coverage (99% and 87%) and sinus tarsi impingement is considerably improved (10%).

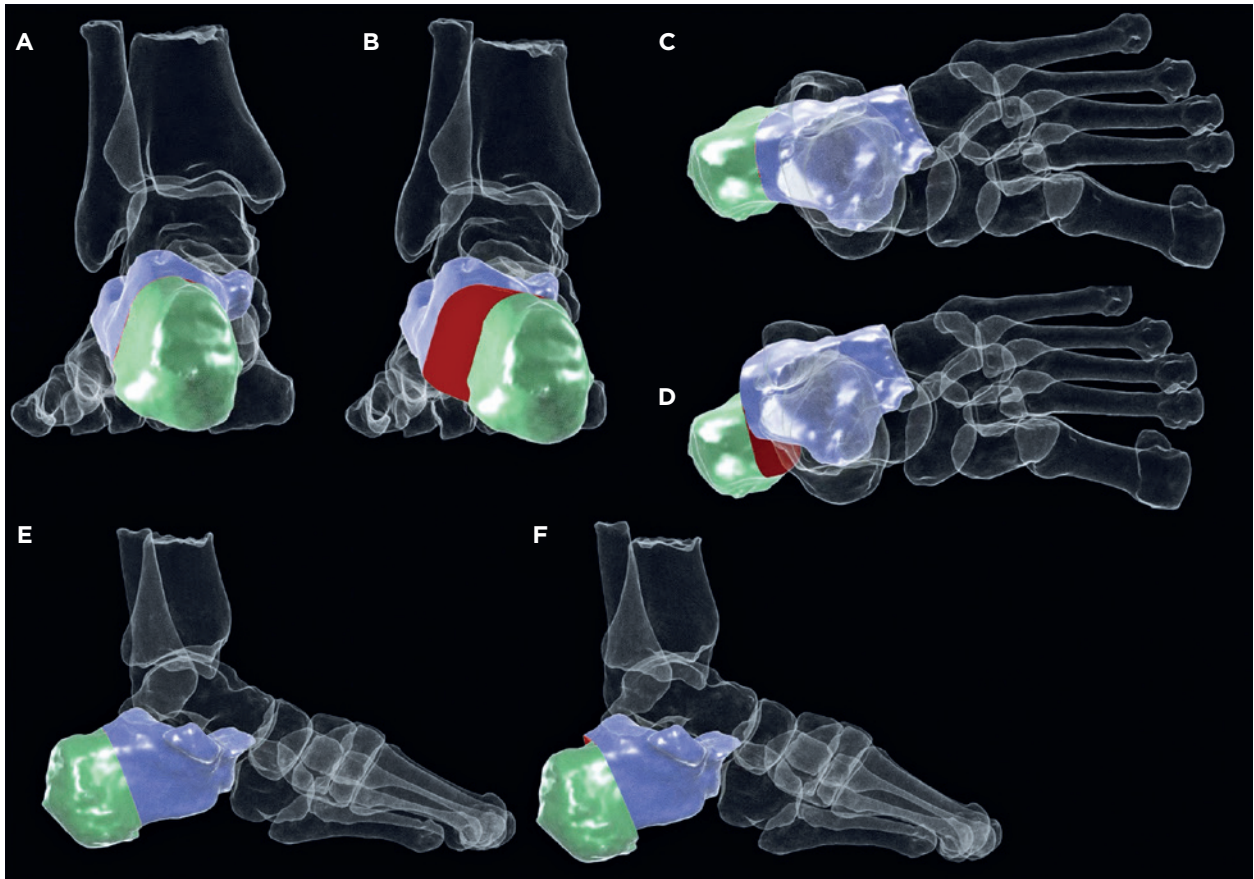


**Figure 6.** Example of preoperative planning of a medial displacement calcaneal osteotomy in a progressive collapsing foot deformity. Coronal (A; B), axial (C; D), and sagittal (E; F) reconstruction images comparing the overall alignment and specific angular and metric relations between bones. Semi-automatic angles can be easily measured in preoperative and postoperative assessments. Even an isolated hindfoot osteotomy can affect different aspects and areas of the foot and ankle.




**Figure 7.** Example of a progressive collapsing foot deformity patient classified as 1ABC presenting with significant posterior tibial tendon degeneration and a viable muscle unit that underwent surgical treatment. Preoperatively (A), sinus tarsi impingement, talonavicular uncoverage, and first tarsometatarsal joint instability are noted. At the two-year follow-up visit (B), after a 10 mm medial displacement calcaneal osteotomy, a 10 mm Lapicotton, posterior tibial tendon reconstruction using hamstring allograft, and a gastrocnemius recession. The capability of the first ray to derotate the hindfoot and correct the talonavicular uncoverage (midfoot abduction) is appreciated.

## Conclusions

Scientific advancements drive humanity. Health sciences are not different, due to our continuous search to offer our patients the best treatment. Substantial information produced in the last decades was detrimental to the development of PCFD understanding. Technology has provided us with expanded perceptions on how the disease behaves and

presents itself. Impact on treatment is also starting to be shown. Although much of these methods are not available in developing countries, concepts and produced data can be applied in clinical practice using existing and resourceful tools. Knowledge will always be the most reliable instrument in the hands of a surgeon and knowledge has no geographical or financial background.

**Authors' contributions:** Each author contributed individually and significantly to the development of this article: NSBM \*(<https://orcid.org/0000-0003-1067-727X>) Conceived and planned the activity that led to the study, wrote the article, participated in the review process; KD \*(<https://orcid.org/0000-0002-8061-4453>), and CCN \*(<https://orcid.org/0000-0001-6037-0685>) Bibliographic review, participated in the review process. All authors read and approved the final manuscript.\*ORCID (Open Researcher and Contributor ID) 

## References

1. Myerson MS, Thordarson D, Johnson JE, Hintermann B, Sangeorzan BJ, Deland JT, et al. Classification and Nomenclature: Progressive Collapsing Foot Deformity. *Foot Ankle Int.* 2020;41(10):1271-6
2. de Cesar Netto C, Deland JT, Ellis SJ. Guest Editorial: Expert Consensus on Adult-Acquired Flatfoot Deformity. *Foot Ankle Int.* 2020;41(10):1269-71.
3. Mansur NS, Lalevée M, Vivtcharenko V, Carvalho K, Dibbern KN, Deland JT, et al. Predictors of Deformity in Patients with Progressive Collapsing Foot Deformity and Valgus of the Ankle. *Foot Ankle Orthop.* 2022;7(2):2473011421S00538.
4. Sangeorzan BJ, Hintermann B, de Cesar Netto C, Day J, Deland JT, Ellis SJ, et al. Progressive Collapsing Foot Deformity: Consensus on Goals for Operative Correction. *Foot Ankle Int.* 2020;41(10):1299-1302.
5. Sangeorzan A, Sangeorzan B. Subtalar Joint Biomechanics: From Normal to Pathologic. *Foot Ankle Clin.* 2018;23(3):341-52.
6. Apostle KL, Coleman NW, Sangeorzan BJ. Subtalar joint axis in patients with symptomatic peritalar subluxation compared to normal controls. *Foot Ankle Int.* 2014;35(11):1153-8.
7. Dibbern KN, Behrens A, Mansur NSB, Carvalho K, Lalevée M, Kim KC, et al. Evaluation of Automated Coverage and Distance Mapping Selections to Improve Reliability and Clinical Utility of 3D Weightbearing CT Assessments. *Foot Ankle Orthop.* 2022;7(4).
8. Schmidt E, Kim KC, Carvalho K, Dibbern KN, Cychosz C, Mansur NSB, et al. The Role of the Transverse Arch in Progressive Collapsing Foot Deformity (PCFD): A Retrospective Case Control Study. *Foot Ankle Orthop.* 2022;7(4):2473011421S00924.
9. Lintz F. *Technology of Weight Bearing Cone Beam Computed Tomography.* Springer International Publishing; 2020. p. 241-7.
10. Lintz F, de Cesar Netto C, Barg A, Burssens A, Richter M, Weight Bearing CTISG. *EFORT Open Rev.* 2018;3(5):278-86.
11. de Cesar Netto C, Schon LC, Thawait GK, da Fonseca LF, Chinanuvathana A, Zbijewski WB, et al. Flexible Adult Acquired Flatfoot Deformity: Comparison Between Weight-Bearing and Non-Weight-Bearing Measurements Using Cone-Beam Computed Tomography. *J Bone Joint Surg Am.* 2017;99(18):e98.
12. Netto CdC, Silva TA, Li S, Dibbern KN, Mansur NS, Lintz F, et al. Posterior vs. Middle Facet of the Subtalar Joint: The Search for an Early Sign of Peritalar Subluxation and Progressive Flatfoot Deformity. *Foot Ankle Orthop.* 2020;5(4):2473011420S00035.
13. Mansur NSB, Lalevée M, Shamrock A, Lintz F, de Carvalho KAM, de Cesar Netto C. Decreased Peritalar Subluxation in Progressive Collapsing Foot Deformity with Ankle Valgus Tilting. *JBJS Open Access.* 2023;8(4):e23.00025.
14. Behrens A, Dibbern K, Lalevée M, Alencar Mendes De Carvalho K, Lintz F, Barbachan Mansur NS, et al. Coverage maps demonstrate 3D Chopart joint subluxation in weightbearing CT of progressive collapsing foot deformity. *Scientific Reports.* 2022;12(1):19367.
15. Dibbern KN, Li S, Vivtcharenko V, Auch E, Lintz F, Ellis SJ, et al. Three-Dimensional Distance and Coverage Maps in the Assessment of Peritalar Subluxation in Progressive Collapsing Foot Deformity. *Foot Ankle Int.* 2021;42(6):757-67.
16. de Cesar Netto C, Barbachan Mansur NS, Lalevée M, Carvalho KAMd, Godoy-Santos AL, Kim KC, et al. Effect of Peritalar Subluxation Correction for Progressive Collapsing Foot Deformity on Patient-Reported Outcomes. *Foot Ankle Int.* 2023;44(11):1128-41.
17. Ananthakrisnan D, Ching R, Tencer A, Hansen ST, Jr., Sangeorzan BJ. Subluxation of the talocalcaneal joint in adults who have symptomatic flatfoot. *J Bone Joint Surg Am.* 1999;81(8):1147-54.
18. de Cesar Netto C, Godoy-Santos AL, Saito GH, Lintz F, Siegler S, O'Malley MJ, et al. Subluxation of the Middle Facet of the Subtalar Joint as a Marker of Peritalar Subluxation in Adult Acquired Flatfoot Deformity: A Case-Control Study. *J Bone Joint Surg Am.* 2019;101(20):1838-44.
19. de Cesar Netto C, Silva T, Li S, Mansur NS, Auch E, Dibbern K, et al. Assessment of posterior and middle facet subluxation of the subtalar joint in progressive flatfoot deformity. *Foot Ankle Int.* 2020;41(10):1190-7.
20. Conti MS, Ellis SJ. Weight-bearing CT Scans in Foot and Ankle Surgery. *J Am Acad Orthop Surg.* 2020;28(14):e595-e603.
21. de Cesar Netto C, Myerson MS, Day J, Ellis SJ, Hintermann B, Johnson JE, et al. Consensus for the Use of Weightbearing CT in the Assessment of Progressive Collapsing Foot Deformity. *Foot Ankle Int.* 2020;41(10):1277-82.
22. Lalevée M, Barbachan Mansur NS, Rojas EO, Lee HY, Ahrenholz SJ, Dibbern KN, et al. Prevalence and pattern of lateral impingements

- in the progressive collapsing foot deformity. *Arch Orthop Trauma Surg.* 2023;143(1):161-8.
23. de Cesar Netto C, Saito GH, Roney A, Day J, Greditzer H, Sofka C, et al. Combined weightbearing CT and MRI assessment of flexible progressive collapsing foot deformity. *Foot Ankle Surg.* 2021;27(8):884-891.
  24. Hintermann B, Deland JT, de Cesar Netto C, Ellis SJ, Johnson JE, Myerson MS, et al. Consensus on Indications for Isolated Subtalar Joint Fusion and Naviculocuneiform Fusions for Progressive Collapsing Foot Deformity. *Foot Ankle Int.* 2020;41(10):1295-8.
  25. Malicky ES, Crary JL, Houghton MJ, Agel J, Hansen ST, Jr., Sangeorzan BJ. Talocalcaneal and subfibular impingement in symptomatic flatfoot in adults. *J Bone Joint Surg Am.* 2002; 84(11):2005-9.
  26. Henry JK, Shakked R, Ellis SJ. Adult-Acquired Flatfoot Deformity. *Foot Ankle Orthop.* 2019;4(1):2473011418820847.
  27. Thordarson D, Schon LC, de Cesar Netto C, Deland JT, Ellis SJ, Johnson JE, et al. Consensus for the Indication of Lateral Column Lengthening in the Treatment of Progressive Collapsing Foot Deformity. *Foot Ankle Int.* 2020;41(10):1286-8.
  28. Ellis SJ, Johnson JE, Day J, de Cesar Netto C, Deland JT, Hintermann B, et al. Titrating the Amount of Bony Correction in Progressive Collapsing Foot Deformity. *Foot Ankle Int.* 2020;41(10):1292-5.
  29. Whitelaw K, Shah S, Hagemeyer NC, Guss D, Johnson AH, DiGiovanni CW. Fusion Versus Joint-Sparing Reconstruction for Patients With Flexible Flatfoot. *Foot Ankle Spec.* 2020; 15(2):150-7.
  30. Mann RA, Beaman DN, Horton GA. Isolated subtalar arthrodesis. *Foot Ankle Int.* 1998;19(8):511-9.
  31. Barbachan Mansur NS, Lalevée M, Lee HY, Ehret A, Fayed A, Mann TS, et al. Influence of Weightbearing Computed Tomography in the Progressive Collapsing Foot Deformity Classification System. *Foot Ankle Int.* 2023;44(2):125-9.
  32. Lee HY, Barbachan Mansur NS, Lalevée M, Dibbern KN, Myerson MS, Ellis SJ, et al. Intra- and interobserver reliability of the new classification system of progressive collapsing foot deformity. *Foot Ankle Int.* 2022;43(4):582-9.
  33. Gross CE, Jackson JB, 3rd. The Importance of the Medial Column in Progressive Collapsing Foot Deformity: Osteotomies and Stabilization. *Foot Ankle Clin.* 2021;26(3):507-21.
  34. Johnson JE, Sangeorzan BJ, de Cesar Netto C, Deland JT, Ellis SJ, Hintermann B, et al. Consensus on Indications for Medial Cuneiform Opening Wedge (Cotton) Osteotomy in the Treatment of Progressive Collapsing Foot Deformity. *Foot Ankle Int.* 2020; 41(10):1289-91.
  35. de Cesar Netto C, Ahrenholz S, Iehl C, Vivtcharenko V, Schmidt E, Lee H, et al. LapiCotton technique in the treatment of progressive collapsing foot deformity. *J Foot Ankle.* 2020;14(3):301-8.
  36. De Cesar Netto C, Ehret A, Walt J, Chinelati RMK, Dibbern K, De Carvalho KAM, et al. Early results and complication rate of the LapiCotton procedure in the treatment of medial longitudinal arch collapse: a prospective cohort study. *Arch Orthop Trauma Surg.* 2023;143(5):2283-95.
  37. Conti MS, Garfinkel JH, Kunas GC, Deland JT, Ellis SJ. Postoperative Medial Cuneiform Position Correlation With Patient-Reported Outcomes Following Cotton Osteotomy for Reconstruction of the Stage II Adult-Acquired Flatfoot Deformity. *Foot Ankle Int.* 2019;40(5):491-8.
  38. Metzl JA. Naviculocuneiform Sag in the Acquired Flatfoot: What to Do. *Foot Ankle Clin.* 2017;22(3):529-44.
  39. Hunt KJ, Farmer RP. The Undercorrected Flatfoot Reconstruction. *Foot Ankle Clin.* 2017;22(3):613-24.
  40. Kadakia AR, Kelikian AS, Barbosa M, Patel MS. Did Failure Occur Because of Medial Column Instability That Was Not Recognized, or Did It Develop After Surgery? *Foot Ankle Clin.* 2017;22(3):545-62.
  41. Day J, de Cesar Netto C, Nishikawa DRC, Garfinkel J, Roney A, M JOM, et al. Three-Dimensional Biometric Weightbearing CT Evaluation of the Operative Treatment of Adult-Acquired Flatfoot Deformity. *Foot Ankle Int.* 2020;41(8):930-6.
  42. Bernasconi A, de Cesar Netto C, Barg A, Burssens A, Richter M, Lintz F, et al. AAFD: Conventional Radiographs are not Enough! I Need the Third Dimension. *Tech Foot Ankle Surg.* 2019;18(3):109-15.
  43. de Cesar Netto C, Bang K, Mansur NS, Garfinkel JH, Bernasconi A, Lintz F, et al. Multiplanar Semiautomatic Assessment of Foot and Ankle Offset in Adult Acquired Flatfoot Deformity. *Foot Ankle Int.* 2020;41(7):839-48.
  44. Lintz F, Barton T, Millet M, Harries WJ, Hepple S, Winson IG. Ground Reaction Force Calcaneal Offset: A new measurement of hindfoot alignment. *Foot Ankle Surg.* 2012;18(1):9-14.
  45. Zhang JZ, Lintz F, Bernasconi A, Weight Bearing CTISG, Zhang S. 3D Biometrics for Hindfoot Alignment Using Weightbearing Computed Tomography. *Foot Ankle Int.* 2019;40(6):720-6.
  46. Lintz F, Welck M, Bernasconi A, Thornton J, Cullen NP, Singh D, et al. 3D Biometrics for Hindfoot Alignment Using Weightbearing CT. *Foot Ankle Int.* 2017;38(6):684-9.
  47. Rojas EO, Barbachan Mansur NS, Dibbern K, Lalevée M, Auch E, Schmidt E, et al. Weightbearing Computed Tomography for Assessment of Foot and Ankle Deformities: The Iowa Experience. *Iowa Orthop J.* 2021;41(1):111-9.
  48. Lintz F, Bernasconi A, Li S, Lalevée M, Fernando C, Barg A, et al. Diagnostic accuracy of measurements in progressive collapsing foot deformity using weight bearing computed tomography: A matched case-control study. *Foot Ankle Surg.* 2022;28(7):912-8.
  49. Lintz F, Mast J, Bernasconi A, Mehdi N, de Cesar Netto C, Fernando C, et al. 3D, Weightbearing Topographical Study of Periprosthetic Cysts and Alignment in Total Ankle Replacement. *Foot Ankle Int.* 2020;41(1):1-9.
  50. Jasper R, Stebral H, Mallavarapu V, Talaski G, Schmidt E, Fayed A, et al. Foot and ankle offset in the setting of severe rotational foot and ankle deformities. *J Foot Ankle.* 2022;16(3):215-21.
  51. Wang LI, Greenspan M, Ellis R. Validation of bone segmentation and improved 3-D registration using contour coherency in CT data. *IEEE Trans Med Imaging.* 2006;25(3):324-34.
  52. Tsao J, Chiodo CP, Williamson DS, Wilson MG, Kikinis R. Computer-assisted quantification of periaxial bone rotation from X-ray CT. *J Comput Assist Tomogr.* 1998;22(4):615-20.
  53. Ortolani M, Leardini A, Pavani C, Scicolone S, Girolami M, Bevoni R, et al. Angular and linear measurements of adult flexible flatfoot via weight-bearing CT scans and 3D bone reconstruction tools. *Sci Rep.* 2021;11(1):16139.
  54. de Carvalho KAM, Mallavarapu V, Ehret A, Dibbern K, Lee HY, Barbachan Mansur NS, et al. The Use of Advanced Semiautomated Bone Segmentation in Hallux Rigidus. *Foot Ankle Orthop.* 2022; 7(4):24730114221137597.
  55. de Carvalho KAM, Behrens A, Mallavarapu V, Jasper R, Mansur NSB, Lalevée M, et al. Automated three-dimensional distance and coverage mapping of hallux valgus: a case-control study. *J Foot Ankle.* 2022;16(1):41-5.
  56. Dibbern K, Talaski G, Schmidt E, Jasper R, Mallavarapu V, Jones M, et al. Ankle syndesmotic instability assessment using a three-dimensional distance mapping algorithm: a cadaveric pilot WBCT study. *J Foot Ankle.* 2022;16(3):190-4.



57. Richter M, Zech S, Naef I, Duerr F, Schilke R. Automatic software-based 3D-angular measurement for weight-bearing CT (WBCT) is valid. *Foot Ankle Surg.* 2022;28(7):868-71.
58. Behrens A, Dibbern KN, Mansur NSB, Ehret A, Chen N, Stebral HJ, et al. Chopart Peritalar Subluxation in Progressive Collapsing Foot Deformity Assessed by Three- Dimensional Coverage Maps. *Foot Ankle Orthop.* 2022;7(4):2473011421S00580.
59. Dibbern K, Vivtcharenko V, Salomao Barbachan Mansur N, Lalevée M, Alencar Mendes de Carvalho K, Lintz F, et al. Distance mapping and volumetric assessment of the ankle and syndesmotric joints in progressive collapsing foot deformity. *Sci Rep.* 2023;13(1):4801.
60. Efrima B, Barbero A, Ramalingam K, Indino C, Maccario C, Usulli FG. Three-Dimensional Distance Mapping to Identify Safe Zones for Lateral Column Lengthening. *Foot Ankle Int.* 2023;44(10):1061-9.
61. Nunes GA, Carvalho KAM, Mansur NSB, Kim KC, Chrea B, Mann TS, et al. Semi-Automatic 3D Assessment of Zadek Osteotomy Effects. *Foot Ankle Orthop.* 2023;8(4):2473011423S00407.
62. Karaismailoglu B, Peiffer M, Sharma S, Burssens A, Waryasz G, Guss D, et al. Effect of Dorsal Closing Wedge Calcaneal Osteotomy on Foot Alignment and Biomechanics in Patients with Insertional Achilles Tendinopathy. *Foot Ankle Orthop.* 2023;8(4).
63. Lintz F, Beaudet P, Richardi G, Brilhault J. Weight-bearing CT in foot and ankle pathology. *Orthop Traumatol Surg Res.* 2021;107(1S):102772.
64. Efrima B, Dahmen J, Barbero A, Benady A, Maccario C, Indino C, et al. Enhancing precision in osteochondral lesions of the talus measurements and improving agreement in surgical decision-making using weight-bearing computed tomography and distance mapping. *Knee Surg Sports Traumatol Arthrosc.* 2024.
65. Peiffer M, Van Den Borre I, Segers T, Ashkani-Esfahani S, Guss D, De Cesar Netto C, et al. Implementing automated 3D measurements to quantify reference values and side-to-side differences in the ankle syndesmosis. *Sci Rep.* 2023;13(1):13774.
66. De Cesar Netto C, Day J, Godoy-Santos AL, Roney A, Barbachan Mansur NS, Lintz F, et al. The use of three-dimensional biometric Foot and Ankle Offset to predict additional realignment procedures in total ankle replacement. *Foot Ankle Surg.* 2022;28(7):1029-34.
67. Faict S, Burssens A, Van Oevelen A, Maeckelbergh L, Mertens P, Buedts K. Correction of ankle varus deformity using patient-specific dome-shaped osteotomy guides designed on weight-bearing CT: a pilot study. *Arch Orthop Trauma Surg.* 2021;143(2):791-9.
68. Heisler L, Vach W, Katz G, Egelhof T, Knupp M. Patient-Specific Instrumentation vs Standard Referencing in Total Ankle Arthroplasty: A Comparison of the Radiologic Outcome. *Foot Ankle Int.* 2022;43(6):741-9.
69. West C, Norrish A, Brassett C, Pasapula C. Evaluation of the heel external rotation test in soft tissue deficiencies associated with adult acquired flatfoot deformity (AAFD). A cadaver sectioning analysis. *Foot (Edinb).* 2023;55:101984.
70. Kim J, Mizher R, Cororaton A, Greditzer H, Sofka C, Ellis S, et al. Cervical Ligament Insufficiency in Progressive Collapsing Foot Deformity: It May Be More Important Than We Know. *Foot Ankle Int.* 2023;44(10):949-57.
71. Lalevée M, Barbachan Mansur NS, Schmidt E, Carvalho K, Vandellune C, Bernasconi A, et al. Does tibialis posterior dysfunction correlate with a worse radiographic overall alignment in progressive collapsing foot deformity? A retrospective study. *Foot Ankle Surg.* 2022;28(7):995-1001.
72. Kelly MJ, Casscells ND. Tendon Transfer versus Allograft Reconstruction in Progressive Collapsing Foot Deformity. *Foot Ankle Clin.* 2021;26(3):465-71.
73. Conti MS, Chan JY, Do HT, Ellis SJ, Deland JT. Correlation of postoperative midfoot position with outcome following reconstruction of the stage II adult acquired flatfoot deformity. *Foot Ankle Int.* 2015;36(3):239-47.
74. Nishikawa DRC, Duarte FA, Saito GH, de Miranda BR, Fenelon EJA, Prado MP. Is first metatarsal shortening correlated with clinical and functional outcomes following the Lapidus procedure? *Int Orthop.* 2021; 45(11):2927-31.
75. Busch A, Wegner A, Haversath M, Brandenburger D, Jäger M, Beck S. First ray alignment in Lapidus arthrodesis - Effect on plantar pressure distribution and the occurrence of metatarsalgia. *Foot (Edinb).* 2020;45:101686.
76. Miniaci-Coxhead SL, Weisenthal B, Ketz JP, Flemister AS. Incidence and Radiographic Predictors of Valgus Tibiotalar Tilt After Hindfoot Fusion. *Foot Ankle Int.* 2017;38(5):519-25.
77. Plaass C, Louwerens JW, Claassen L, Ettinger S, Yao D, Lerch M, et al. Treatment concepts for pes planovalgus with concomitant changes of the ankle joint. *Orthopade.* 2020;49(11):991-9.
78. Dodd A, Daniels TR. Total Ankle Replacement in the Presence of Talar Varus or Valgus Deformities. *Foot Ankle Clin.* 2017;22(2): 277-300.
79. Kuestermann H, Ettinger S, Yao D, Schwarze M, Plaass C, Stukenborg-Colsman C, et al. Biomechanical evaluation of naviculocuneiform fixation with lag screw and locking plates. *Foot Ankle Surg.* 2021; 27(8):911-9.
80. Partio N, Mattila VM, Mäenpää H. Bioabsorbable vs. titanium screws for first tarsometatarsal joint arthrodesis: An in-vitro study. *J Clin Orthop Trauma.* 2020;11(3):448-52.
81. Romeo G, Bianchi A, Cerbone V, Parrini MM, Malerba F, Martinelli N. Medial Cuneiform Opening Wedge Osteotomy for Correction of Flexible Flatfoot Deformity: Trabecular Titanium vs. Bone Allograft Wedges. *Biomed Res Int.* 2019;2019:1472471.
82. Fonseca LF, Baumfeld D, Mansur N, Nery C. Deltoid Insufficiency and Flatfoot—Oh Gosh, I'm Losing the Ankle! What Now? *Tech Foot Ankle Surg.* 2019;18(4):202-7.
83. Nery C, Lemos AVKC, Raduan F, Mansur NSB, Baumfeld D. Combined spring and deltoid ligament repair in adult-acquired flatfoot. *Foot Ankle Int.* 2018;39(8):903-7.